ISSN: 2347-3487

Signal-to-Noise Ratio importance in Apparent Diffusion Coefficient measurements using Diffusion-Weighted Echo-Planar-Imaging scans

Cristiano Biagini[1], Martina De Michele, [2]Andrea Pratesi, [3]Francesco Mungai[4], Margherita Betti[5], Giana Izzo[6], Carlo Biagini[1], Luigi Natale[6]

[1]Department of Radiology, Centro OncologicoFiorentino, Sesto Fiorentino, Florence(Italy)

cristiano.biagini@lacittadellasalute.it

[2]Fisica Sanitaria, University of Florence, Florence (Italy)

mdimichele@gmail.com

[2]State Hospital "Misericordia e Dolce", Prato (Italy)

a.pratesi@gmail.com

[4]Department of Experimental and Clinical Biomedical Sciences, Radiodiagnostic Unit n.2, University of Florence, Florence (Italy)

f.mungai@gmail.com

[5]Radiotherapy Unit, Centro OncologicoFiorentino, Sesto Fiorentino, Florence, Italy

margherita.betti@lacittadellasalute.it

[6]Department of Radiological Sciences, UniversitàCattolica "SacroCuore", Rome (Italy)

gianaizzo@gmail.it

[1]Department of Radiology, Centro OncologicoFiorentino, Sesto Fiorentino, Florence(Italy)

carlo.biagini@lacittadellasalute.it

[6]Department of Radiological Sciences, UniversitàCattolica "SacroCuore", Rome (Italy)

lnatale@rm.unicatt.it

Correspondingauthor: Cristiano Biagini

Indirizzo: Cristiano Biaginic/o Centro Oncologico Fiorentino (C.F.O.), Via Attilio Ragionieri 101, 50013 Sesto Fiorentino (FI), Italy

Tel: +39.0555301914 - +39.3496272041 Fax: +39.0555301102

E-mail: cristiano.biagini@lacittadellasalute.it

ABSTRACT

Purpose: To define experimental grounds for Apparent Diffusion Coefficient (ADC) measurements using Spin-Echo Diffusion-Weighted Echo-Planar (SE-DW-EPI) sequences, as a function of Signal-to-Noise Ratio (SNR).

Methods: multiple multi-b SE-DW-EPI scans with the same parameters but the lipid suppression technique have been compared on water phantom with a 3T MRI equipment. The SNR has been estimated using the method of difference. Images have been analyzed manually, comparing the signal intensities at different b-values.

Results: All measurements show a high repeatability and strong self-consistency. A significant dependence of the ADC on SNR has been shown, and its lowest limitto obtain reliable quantitative answers has been stated.

Conclusion: ADC measurements in vivo must be carefully designed to avoid systematic errors during acquisition and post-processing due to low SNR.

INDEXING TERMS/KEYWORDS

Diffusion Magnetic Resonance Imaging, Artifacts, MRI Physics, fat suppression techniques

ACADEMIC DISCIPLINE AND SUB-DISCIPLINES

Physics, Radiology

TYPE (METHOD/APPROACH)

EXPERIMENTAL PHANTOM STUDY

ISSN: 2347-3487

INTRODUCTION

Diffusion-weighted imaging (DWI) has become an indispensable tool in clinical routine, both in neuro and in body MR imaging [1-3]. DWI has the ability to extract information about tissue micro-structure from MR signal intensities, giving the Radiologist useful details to assess the presence or absence of abnormalities, and even their nature. Its application ranges from treatment monitoring in different physiological regions [2,4-5] to functional characterization to tissue geometry as in Diffusion Tensor Imaging [2].

As well known, the imaging technique used for diffusion quantification in vivo, represented by ADC measurements, i.e. the so-called Echo Planar Imaging (EPI), represents the fastest imaging technique, allowing the acquisition of a single bidimensional image in less than 50 ms [6]. Such a high imaging rate has a heavy drawback in the fact that EPI is prone to a number of artifacts [6,7], as its huge sensitivity to type 1 chemical shift (see for example pp. 732-733 in Ref. [6]). Therefore, it is mandatory to suppress the lipid signal in vivo using one of the available fat suppression (FS) techniques; spectrally-selective inversion pulses, both adiabatic (as in SPectrally Adiabatic Inversion Recovery, SPAIR) or not (as in the conventional Fat Saturation, FatSat, CHESS or SPIR), non spectrally-selective inversion pulses (Inversion Recovery, IR) or selective excitation of water protons with composite pulses (Water Excitation, WE).

Each of those techniques uses RF pulses with different duration, envelope and intensity, and also has different spoilers and crushers contributions. Actually, all of them found their application domain in different anatomic districts: the choice is usually dictated by technical reasons as the size of the FoV or the importance of field inhomogeneities [6-8].

It has been reported that different FS techniques return “significantly different ADC values” [8] without further explanation. In our opinion, such an ambiguity on a quantitative measurement must be clarified. In fact, should the discrepancy be related to the FS technique itself, the measurement would lose its entire “quantitative” meaning. In this work, we will show that the discrepancy has in effect a common origin, related to the intrinsic SNR of each FS technique, and so care must be paid to the correct choice of the technique and the corresponding diffusion sequence parameters, as the *b*-value.

A following paper will discuss the intrinsic distortion of the signal intensity curve as a function of the *b* value, due to the presence of the FS pulses itself (to be published).

METHODS

Measurements have been realized on a 3T MRI equipment (Siemens Verio) with a 12-channel Head Matrix coil, using a phantom realized by the Medical Physics Unit of the AziendaOspedalieraUniversitaria di Careggi (AOUC), in Florence (Italy) [9]: it is a Plexiglas cylinder filled with an aqueous solution of Agarose (1.2% weight fraction) with a diffusion coefficient $D \approx 1.95 * 10^{-3}$ mm^2/s at 20 Celsius degrees; to take into account thermal effects due to RF deposition, a alcohol thermometer was inserted in the cylinder, in close contact with the solution.

The phantom has been kept inside the magnet room at all times, in order to minimize its movement and to ensure thermal equilibrium with the environment. We have verified that the temperature of the solution in the phantom did not show any variation before, during and after the measurement session.

The measurements have been realized at the beginning and/or at the end of an examination session, in order to average over the stress of the acquisition and reconstruction electronics; the order of execution of the pulse sequences has been changed in different measurement sessions to average on the possible heating of the phantom solution (even if the Specific Absorption Rate (SAR) of SE-DW-EPI scans is close to zero) and of the acquisition electronics; care has been paid in the phantom positioning to repeat the sequences in the same geometry during different sessions; after positioning at the magnet isocenter, the phantom has been left to rest for about twenty minutes before starting the acquisition to eliminate every possible convection motion of the solution; a typical example of measurement session is represented by the following temporal list of pulse sequences:

1. SE-DW-EPI (No pulse)
2. SE-DW-EPI (SPAIR)
3. SE-DW-EPI (FatSat)
4. SE-DW-EPI (WE)
5. SE-DW-EPI (STIR).

All acquisition results did not show significant variations during every measurement session, demonstrating the high stability of our MR equipment.

Initially, the same SE-DW-EPI sequence with two *b*-values (0, 1000) s/mm^2 has been acquired five times, with a perfect coincidence of all acquisition parameters but the FS technique. The common scan parameters were: *b*=0, 1000; FoV=200 mm; Read Matrix=128; Phase Matrix=128; Phase partial Fourier=7/8; slice thickness/gap=9.0/2.7 mm; number of slices=5; T_R=2000 ms; T_E=90 ms; EPI factor=50; 4 averages; bandwidth=1428 Hz/pixel; iPAT acceleration factor=2; Total scan duration=40”. The FS technique used were: one without RF suppression pulse, two with spectrally selective fat suppression pulse (FatSat, SPAIR), one with a water excitation composite pulse (WE) and the last with a non-spectrally selective fat suppression pulse (IR, T_I=220 ms). This value corresponds to the fat inversion time at 3T for large T_R; taking into account that the T_1 of our phantom is around 1500-2000 ms, the signal drop due to the inversion pulse at T_R=2000 ms corresponds to about 50%, i.e., slightly larger than what expected for water in living tissues (20%); on the other hand, this drop will affect only the absolute value of the signal intensity and not the ADC. More importantly, we will discuss the

results on the SNR at high *b* in comparison to the SNR measured at *b*=0, and therefore its absolute numerical value does not have a deep meaning. The diffusion gradients have been applied consecutively on the three orthogonal encoding directions (phase and read encoding axes, slice selection axis) and an isotropic Trace image has been extracted [6,10,11].

The temperature of the phantom solution has been recorded before and after each sequence, without noticing any change due to RF power deposition. Moreover, we acquired the ADC values in a range between 18.0 and 23.0 Celsius degrees by varying in a controlled way the environmental conditions of the magnet room: we extracted the temperature dependence of the ADC (Fig. 2), corresponding to a variation of (2.42±0.06)% per degree around 20 Celsius degrees in very good agreement with Ref. [9]: using this result, we renormalized all data to the temperature of 20.0 Celsius degrees, taken as the reference temperature in what follows.

In a second run, we analyzed the importance of the SNR on a direct measurement of the ADC: after following the prescriptions reported for the first run, each scan has been repeated twice to estimate reliably the SNR, even in the presence of phased-array coils and parallel imaging techniques [12-16]; the order of the execution of the pulse sequences has been inverted in the second acquisition to average on the possible heating of the phantom solution (even if the Specific Absorption Rate (SAR) of SE-DW-EPI scans is close to zero) and of the acquisition electronics:

1. SE-DW-EPI (SPAIR)
2. SE-DW-EPI (FatSat)
3. SE-DW-EPI (WE)
4. SE-DW-EPI (STIR)
5. SE-DW-EPI (STIR) “bis”
6. SE-DW-EPI (WE) “bis”
7. SE-DW-EPI (FatSat) “bis”
8. SE-DW-EPI (SPAIR) “bis”.

The “no pulse” sequence does not have any application in vivo and we skipped its execution in this run. Each sequence had nominal *b* in the range (0,3000) s/mm^2, with steps of 300 s/mm^2; again, common parameters were: *b*=(0, 300, 600, 900, 1200, 1500, 1800, 2100, 2400, 3000); FoV= 200 mm; Read matrix 128; Phase matrix 64; Phase partial Fourier=7/8; slice thickness/gap=9.0/2.7 mm; number of slices=5; T_R=2600 ms; T_E=116 ms; EPI factor=64; 4 averages; bandwidth=1446 Hz/pixel; iPAT acceleration factor=2; Scan total duration=2’04”. The diffusion gradients have been applied only along the Read direction, after a careful inspection of its greater stability among the various encoding axis [9] on our 3T MRI equipment as a function of *b* (to be published), as shown in Fig. 3.

POST-PROCESSING

In the first run, all images have been analyzed as follows: a ROI containing at least the 80% of the image has been drawn on the central image of the first sequence at *b*=0; the signal intensity has been recorded; copying the ROI on the same image of the other sequences, we have been able to evaluate the ADC values per each fat suppression technique and for each *b* value; the numerical values of the mean signal intensity has been used to calculate the logarithmic intensity ratio $L_b=log(S_0/S_b)$ and then the ADC value as ADC=L_b/b; the same ROI has been copied also on the automated ADC map returned by the equipment and the ADC value has been recorded.

In the second run, we calculate first the arithmetic average (Mean) and the subtraction (Sub) images of each pair of identical sequences; from the new series, we obtain the ADC value as in the first run. We further evaluate the SNR as the ratio of intensity on the Mean image divided by the standard deviation of the Sub image [15]. After temperature renormalization, we have taken the average value of the ADC for the following comparisons.

RESULTS

First of all, it is worth to stress that all measurements have been extremely reproducible for all FS techniques, giving raise to very small standard deviations, in the order of 0.7%, even after temperature renormalization which could introduce by itself a further instability in the data.

The results in the first run of measurements on phantom A are reported in Fig. 4. The error bars represent *three* standard deviations (i.e., more than 99% of the data): the ADC values obtained with the FatSat, SPAIR and WE scans are consistent with each other and with non saturated one, apart for a slight overestimation of the ADC with respect to this scan. The IR scan returns an underestimation of the ADC, and the value is inconsistent with all other saturated scans on the basis on the Student’s test.

In Fig. 5 we reported the diffusion images at *b*=1000 for each FS technique, to show the evident difference in SNR between the frequency-selective techniques (SPAIR, FatSat, WE) and the IR one.

The results of the second run of measurements on the same phantom are summarized in Fig. 6; we reported the ADC values normalized at the value obtained for *b*=300 s/mm^2 as a function of *b*: all curves show a “plateau” till a *b* at which one can observe a “knee”; for higher *b*, the ADC decreases almost linearly.

As the phantom cannot show other diffusion contributions apart the self-diffusive one, the ADC must be a constant as a function of *b*; therefore, any deviation from constancy shall be an artifact.

We will show in the following that it is related to the exponential fall of the SNR with raising *b*, which has been reported in Figs. 7 and 8: comparing Figs. 6 and 8, one can observe that the ADC starts to decrease for all the scans when the SNR falls below a threshold value of about 5. This value corresponds to *b*=1200 for the IR scan, while for the others we found *b*=2100: it is worth to stress that those values are also a function of the underlying diffusion coefficient. For larger *b*, the ADC continues to decrease monotonically, while the SNR shows a plateau.

DISCUSSION

In Fig. 4, we observed a discrepancy between ADC values obtained from scans with different FS techniques. The IR scan has shown a significant underestimation of the ADC; this effect can be related to the rapid fall of the SNR at high *b*-values, as can be observed in Fig. 5.

This result has triggered a second run of measurements on the same phantom, to evaluate the importance of the SNR of the high *b* images: as can be observed in Fig. 7, the SNR strongly depends on the FS technique used, and the IR scan has an intrinsic SNR 4 to 7 times lower than the others on our MRI equipment. As the diffusion measurements depend just on the signal attenuation, which is itself an exponentially decreasing function of the diffusion weighting (i.e., the *b*-value), it is reasonable to expect that there is a *b*-value at which the SNR of the high *b* images becomes too small, and the signal itself comparable to the noise level.

As shown in Fig. 8, we have found a threshold value of 5 for the SNR; below such a threshold, the MRI equipment is acquiring only noise at high *b*, which is obviously constant with respect to *b* itself. As a consequence, the diffusion coefficient *D* cannot be calculated anymore as $D=log(S_0/S_b)/b$: in fact, in this region the logarithmic intensity L_b is a constant and L_b/b is an unphysical linearly decreasing quantity.

The *b*-value at which the threshold is reached depends on the acquisition scan chosen for the measurement and also on the diffusion coefficient of the underlying tissue. We have found an analytic formula for the *b*-value at the threshold b_{thr}, as a function of SNR_0, the signal-to-noise ratio of the specific sequence at *b*=0, and *D*, the underlying diffusion coefficient:

$$b_{thr}(D,SNR_0)=log(SNR_0/5)/D. \quad (1)$$

Eqn. (1) is the main result of this work.

In the IR case, being SNR_0~48 and D~$2.0*10^{-3}$, we obtain b_{thr}~1130. This result is in agreement with our first run of measurements, where the ADC measured by the IR sequence was significantly lower than the ADC obtained with all the other sequences: in fact, the high *b*-value chosen for the experiment (*b*=1000) was in the “critical” region for the IR sequence, where the signal starts to get too close to the threshold.

For the other sequences, one has SNR_0~300 and then b_{thr}~2100. In vivo, the diffusion coefficient is usually smaller than that of the free water and therefore b_{thr} can be significantly higher. Even if this is the case, great care must be paid in the choice of the correct *b*-value in order to avoid errors. Use of Eqn. (1) above can be of help, where it is possible to obtain a coarse estimate of the SNR of the acquisition used and of the diffusion coefficient of the underlying tissue.

Our result can be of importance in vivo: due to the fact that the diffusion coefficient of a tumor is significantly smaller than those of the surrounding normal tissue, the two can have different b_{thr}'s: the normal tissue will have a lower b_{thr} with respect to the tumor. Therefore, if the chosen high *b* falls between the two values, the normal tissue will show an unreal lower ADC, even comparable to the ADC of the tumor, masking its presence or showing a larger lesion; in both cases, one could draw the erroneous conclusion that the tumor itself is not present (false negative) or that it is larger than in the reality (false positive).

CONCLUSION

DWI is a powerful and reproducible tool for the Radiologist. On the other hand, our experiments show that its use must be accompanied by a careful analysis both on the acquisition scan and the post-processing procedure.

Our work shows that care must be paid in order to maintain the SNR above a critical threshold, which we evaluated on our 3T equipment to be around 5, but can differ on other equipments; measurements realized on the same equipment and with the same FS technique on tissues with large differences in diffusivity can be unreliable, if $b>b_{thr}(D)$ for one or more tissues.

ISSN: 2347-3487

FIGURES

Fig. 1: The phantom realized by the Medical Physics Unit of the AOUC of Florence, Italy. It is a plexiglass cylinder, filled with an acqueous solution of Agarose (1.2% weight fraction) with a thermometer in close contact with the solution.

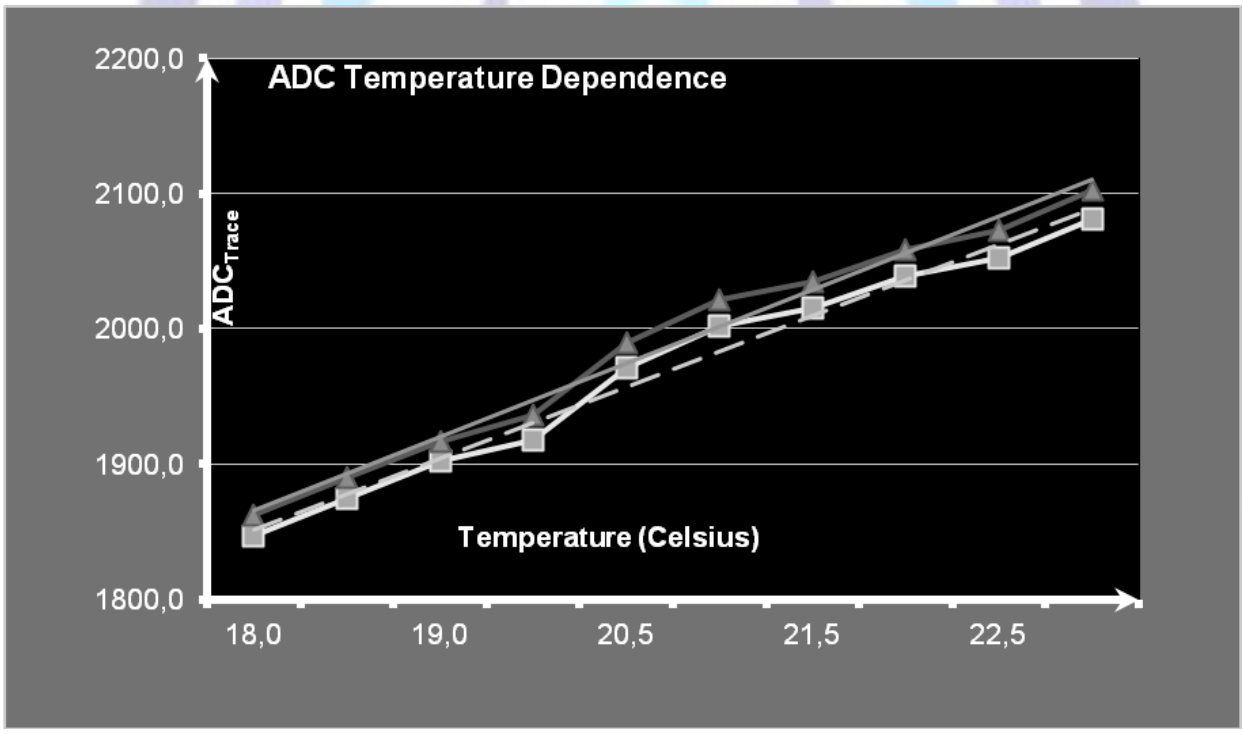

Fig. 2: The temperature dependence of the measured ADC.
The higher values have been calculated by us, by a linear fit of the logarithm of the signal intensities at various b; the lower values have been given by the automated post-processing of the MRI equipment.

ISSN: 2347-3487

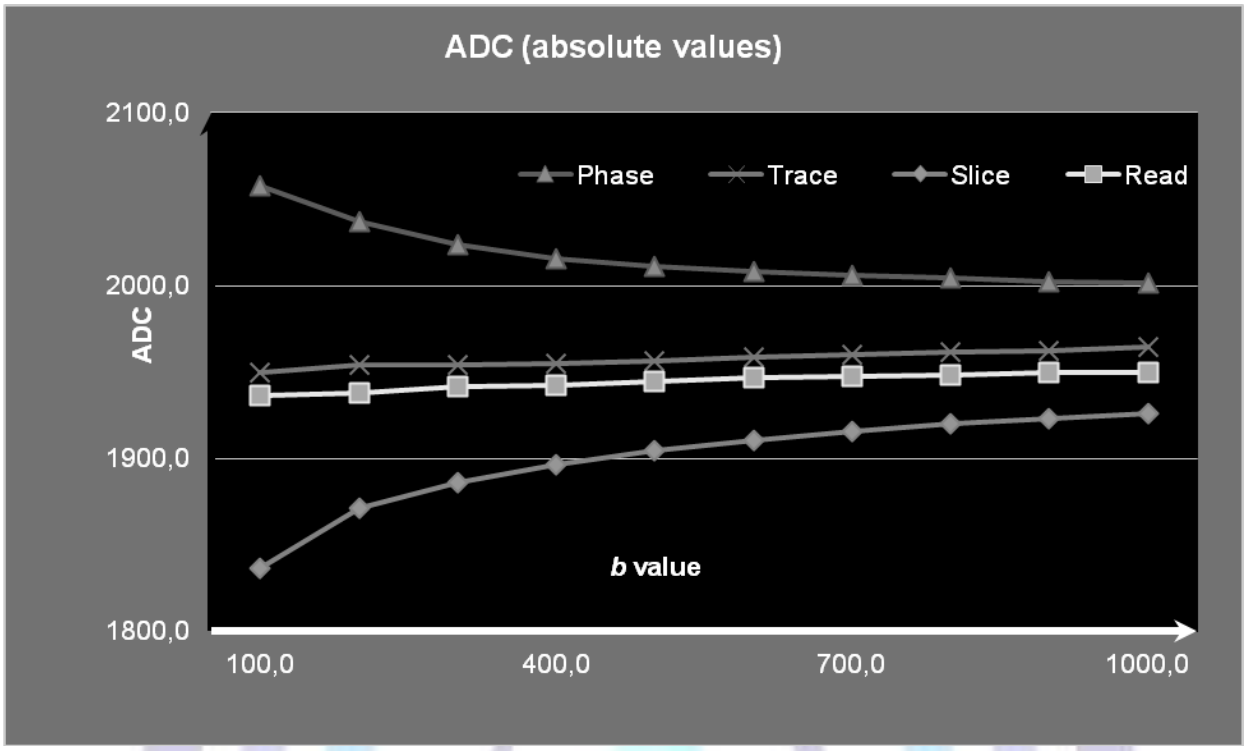

Fig. 3: The ADC value measured along the three spatial encoding directions (Phase, Read and Slice) and for the Trace at b=1000. It is evident the large deviation when the diffusion gradients are applied along the Phase and Slice directions.

The ADC in the Read direction is instead almost constant, showing a small dependence on b. Also the Trace is almost constant: it can be due to an almost exact cancellation of the deviations along the Phase and the Slice gradients.

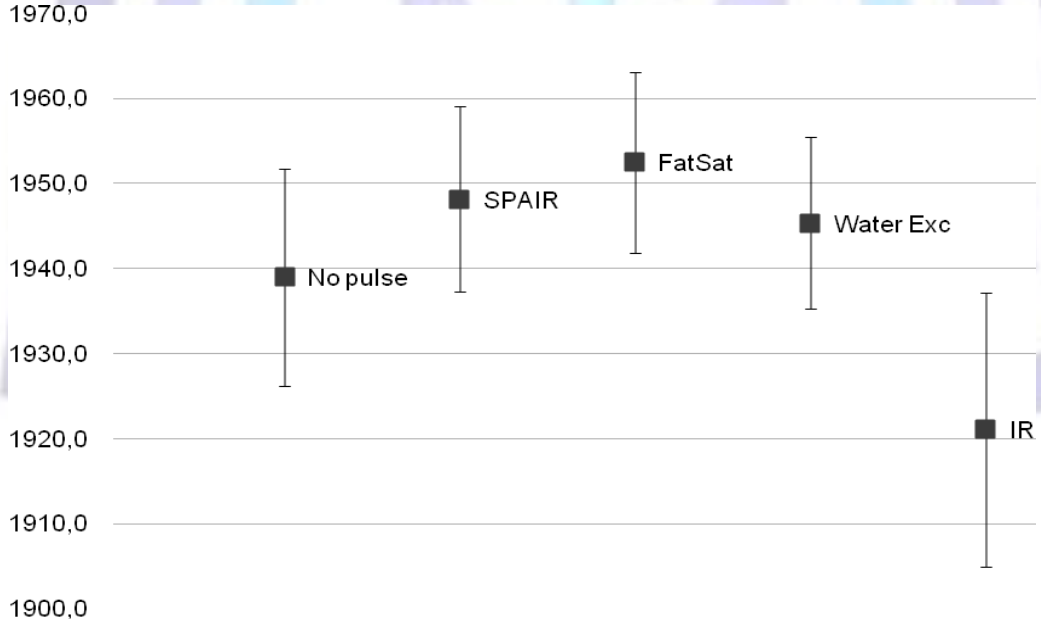

Fig. 4: Five different values of ADC, under the same conditions and with the same scan, apart for different fat saturation techniques: one is non saturated (no RF pulse), three are spectrally selective methods (SPAIR, FatSat, Water Excitation)

and one uses a non spectral selective pulse (Inversion Recovery). It is clearly evident the discrepancy between the non saturated scan and the other results. In particular, the IR-dependent value is barely consistent with all the other techniques.

ISSN: 2347-3487

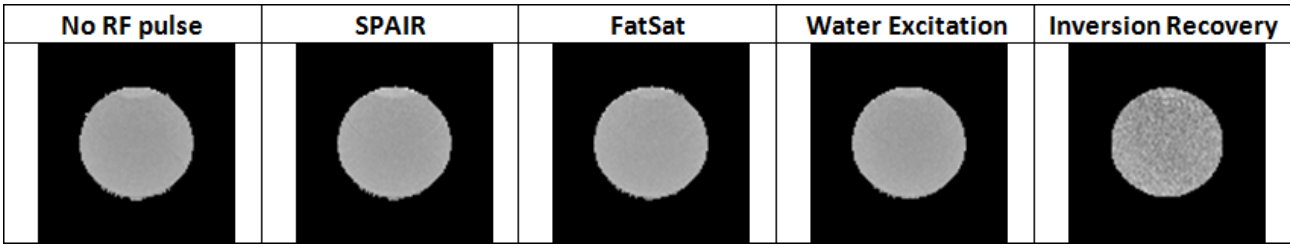

Fig. 5: Five ADC maps from the same DWI sequence apart for the fat saturation technique. It is apparent, even at glance, the discrepancy in the IR ADC map.

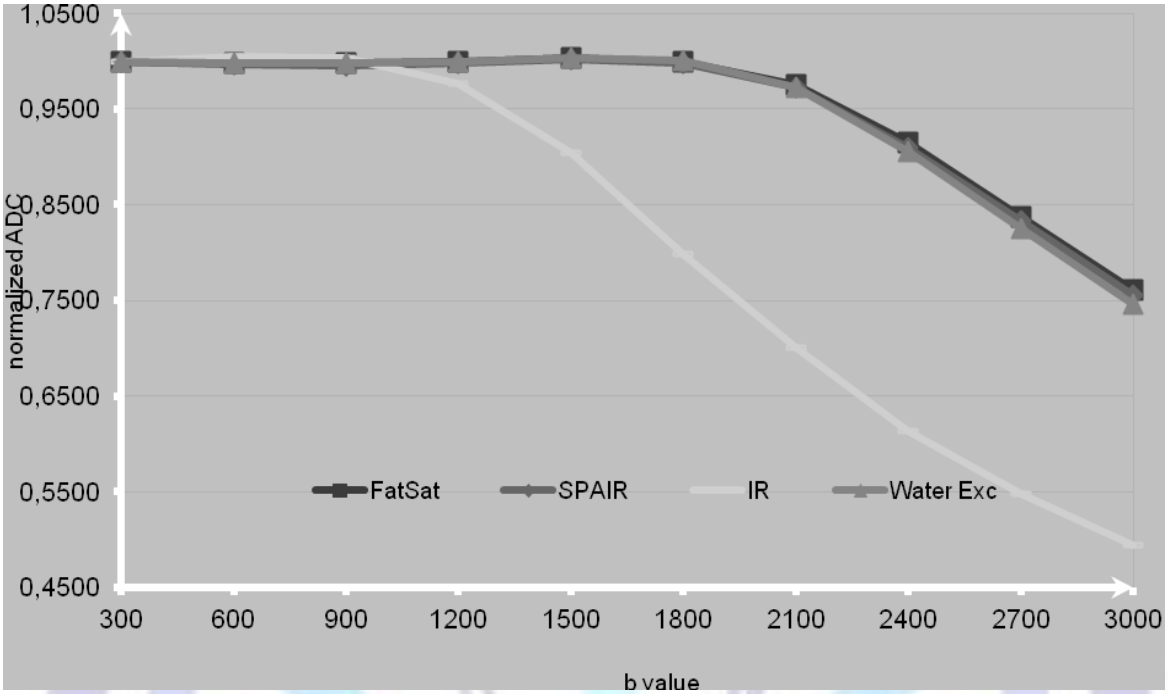

Fig. 6: ADC deviation in multi-b scan due to the fall of SNR at high b-values, for the same scan but with four different fat saturation technique, three spectrally-selective (SPAIR, FatSat, Water Excitation) and one non-spectrally selective (Inversion Recovery).

ISSN: 2347-3487

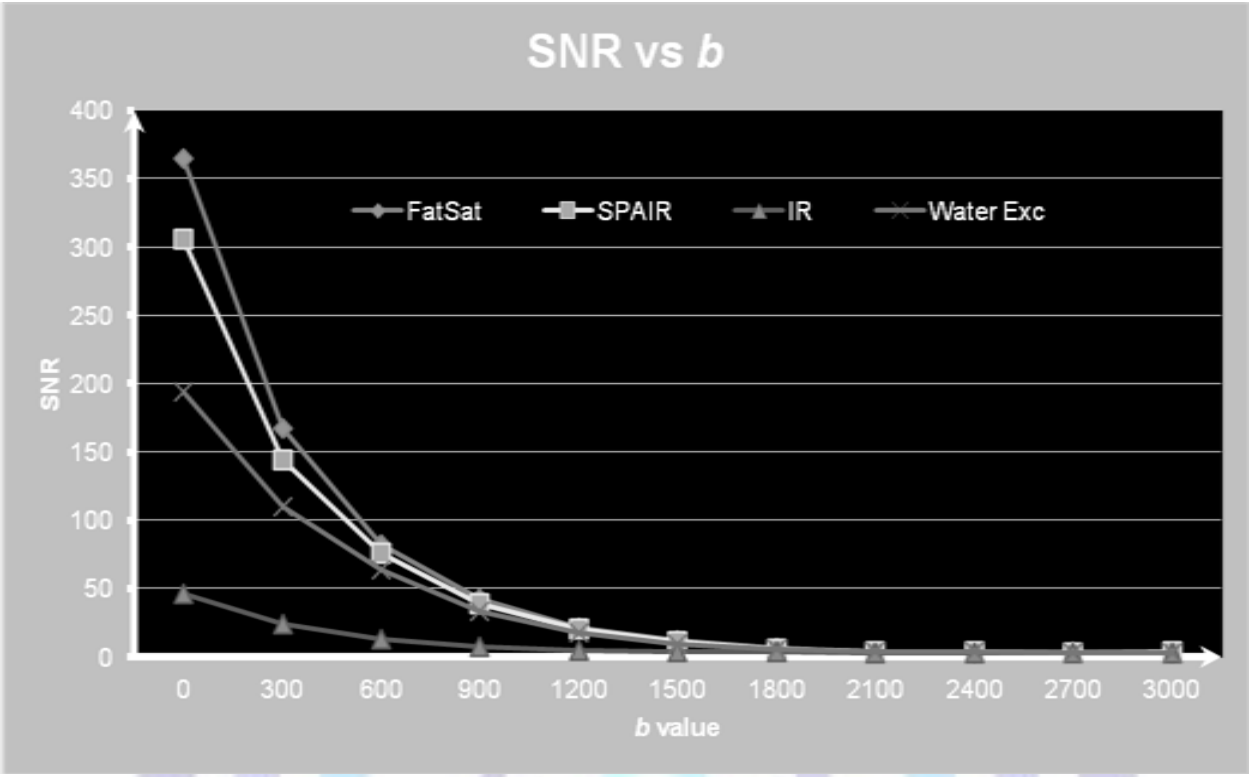

Fig. 7: The SNR as a function of the nominal b-value for all the four fat saturation techniques. It is immediately evident the very low starting value of the Inversion Recovery sequence and its almost immediate saturation below the threshold of reliability (see text).

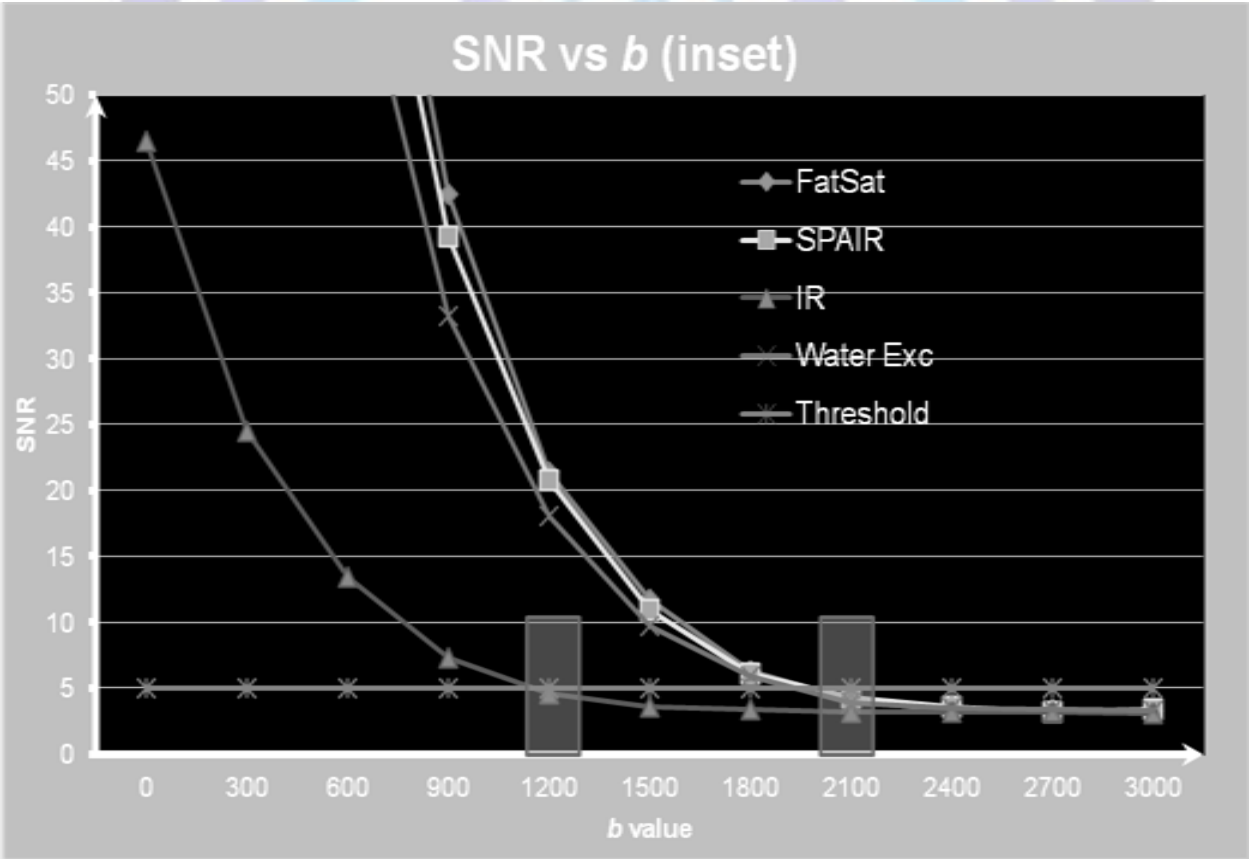

Fig. 8: The detail of the SNR at high b-values for the same scan but with four different fat saturation techniques, three spectrally selective (SPAIR, FatSat, Water Excitation) and a fourth non spectrally selective (Inversion Recovery). The points at b=1200 and 2100 are highlighted, because it is the b-value at which the non spectrally selective saturation sequence and the spectrally selective ones, respectively, fall below the "threshold" value of SNR=5; those points correspond also the "knee" of the ADC curve in Fig. 6.

REFERENCES

[1] Le Bihan D. (2008)Intravoxel Incoherent Motion Perfusion MR Imaging: a Wake-Up Call. *Radiology*; **249**:748-752 and references therein

[2] Moritani T, Ekholm S, Westesson P-L. (2005) Diffusion-Weighted MR Imaging of the Brain, Springer, Berlin-Heidelberg:, , p 229.

[3] Ko DM, Thoeny HC. (2010) Diffusion-Weighted Imaging - Applications in the Body, Springer, Berlin-Heidelberg , p 299.

[4] Cui Y, Zhang XP, Sun YS. (2008) Apparent diffusion coefficient : potential imaging biomarker for prediction and early detection of response to chemoterapy in hepatic metastases. Radiology248:894-900.

[5] Seierstad T, Roe K, Olsen DR. (2007) Noninvasive monitoring of radiation-induced response using proton magnetic resonance speectroscopy and diffusion-weighted magnetic resoance imaging in a colorectal tumor model. Radiotherapy and Oncology85:187-194.

[6] Bernstein MA, King KF, Zhou XJ.(2004) Handbook of MRI pulse sequences, Elsevier Academic Press, San Diego, p 1017.

[7] Tsao J. (2010) Ultrafast imaging: principles, pitfalls, solutions, and applications. Journal of Magnetic Resonance Imaging 32:252-266

[8] Woodhams R, Ramadan S, Stanwell P, Sakamoto S, Hata H, Ozaki M, Kan S, Inoue Y. (2011) Diffusion-weighted imaging of the breast: principles and clinical applications. Radiographics; 31:1059-1084 and references therein.

[9] Colagrande S, Pasquinelli F, Mazzoni LN, Belli G, Virgili G. (2010) MR-Diffusion weighted imaging of healthy liver parenchyma: repeatibility and reproducibility of apparent diffusion coefficient measurement", Journal of Magnetic Resonance Imaging; 31:912-920.

[10] Haacke EM, Brown RW, Thompson MR, Venkatesan R. (1999) Magnetic Resonance Imaging – Physical principles and sequence design. Wiley-Liss, New York , p 914.

[11] Tofts P. (2003) Quantitative MRI of the brain – Measuring changes caused by disease, Wiley & Sons, London, p 650 and references therein.

[12] Pruessmann KP, Weiger M, Scheidegger MB, Boesiger P. (1999) SENSE: Sensitivity encoding for fast MRI. Magnetic Resonance in Medicine 42:952-962.

[13] Wiesinger F, Boesiger P, Pruessmann KP. (2004) Electrodynamics and ultimate SNR in parallel MR imaging. Magnetic Resonance in Medicine 52:376-390

[14] Reeder SB, Wintersperger BJ, Dietrich O, Lanz T, Greiser A, Reiser MF, Glazer GM, Schoenberg SO. (2005) Practical approach to the evaluation of signal-to-noise ratio performance with parallel imaging: application with cardiac imaging and a 32-channel cardiac coil. Magnetic Resonance in Medicine 54:748-754.

[15] Kellmann P, McVeigh ER. (2005) Image reconstruction in SNR units: a general method for SNR measurement. Magnetic Resonance in Medicine 54:1439-1447 and references therein.

[16] Plein S, Ryf S, Schwitter J, Radjenovic A, BoesigerP,Kozerke S. (2007) Dynamic Contrast-Enhanced Myocardial Perfusion MRI Accelerated with k-t SENSE", Magnetic Resonance in Medicine 58:777-785.